Available online at www.CivileJournal.org

Civil Engineering Journal

(E-ISSN: 2476-3055; ISSN: 2676-6957)

Vol. 9, No. 04, April, 2023

Performance Evaluation of Fiber-reinforced Ferroconcrete using Response Surface Methodology

Temitope F. Awolusi [1], Alenoghena I. Ekhasomhi [1], Oluwatobi G. Aluko [2, 3*], Olanike O. Akinkurolere [2], Marc Azab [4], Ahmed Farouk Deifalla [5]

[1] *Department of Civil Engineering, Afe Babalola University, 360231, Ado Ekiti, Nigeria.*

[2] *Department of Civil Engineering, Ekiti State University, 362103, Ado Ekiti, Nigeria.*

[3] *School of Civil Engineering, Universiti Teknologi Malaysia, 81310 Johor, Malaysia.*

[4] *College of Engineering and Technology, American University of the Middle East, Egaila 54200, Kuwait.*

[5] *Structural Engineering and Construction Management Department, Future University in Egypt, 11845, New Cairo, Egypt.*

Received 11 December 2022; Revised 24 February 2023; Accepted 11 March 2023; Published 01 April 2023

Abstract

Fibre-reinforced ferroconcrete is a new-generation type of concrete that has been found to have adequate performance. Global emissions of CO_2 as a result of concrete production have damaged the earth's atmosphere. These emissions, together with construction waste, such as ceramic powder and aluminium waste, are considered one of the most harmful wastes to the environment, eventually leading to pollution. In this study, the fibre-reinforced ferroconcrete (FRFC) contained waste aluminium fibre, cement, ceramic waste powder, corrugated wire mesh, and fine and coarse aggregate. The cement content in the concrete mix was partially replaced with Ceramic Powder (CP) in proportions of 0%, 10%, and 20%, while the Aluminum Fibers (AF) were added in proportions 0, 1, and 2% to the concrete mix. The variation of ceramic powder and aluminium fibres was done using the central composite design of Response Surface Methodology (RSM) to create experimental design points meant to improve the fibre-reinforced ferroconcrete's mechanical performance. The results conclude that the mechanical performance of the FRFC was slightly improved more than conventional concrete, where at 20% replacement of ceramic powder and 1% addition of aluminium fibre to the concrete mix. There was more compressive, flexural, and split tensile strength increase than conventional concrete, with control concrete having strengths of 13.060, 5.720, and 3.110 N/mm^2 and ferroconcrete 15.88, 6.68, and 3.83 N/mm^2 respectively. This was further confirmed with microstructural images. The RSM model, with parameters such as; contour plots, analysis of variance, and optimisation, was used to effectively predict and optimise the responses of the ferroconcrete based on the independent variables (Aluminum fibre and Ceramic Powder) considered. The results of the predicted data show a straight-line linear progression as the coefficient of determination (R^2) tends to 1, indicating that the RSM model is suitable for predicting the response of the variables on the FRFC.

Keywords: Ferroconcrete; RSM-Based Model; Splitting Tensile Strength; Flexural Strength; Concrete Material Optimisation.

1. Introduction

The continuous demand for modern infrastructure by developed and developing nations has increased industrial waste from the construction industry, posing environmental risks and hazards. This rising demand for cement production globally has equally resulted in the depletion of natural resources and an increase in the emission of CO_2, leading to environmental hazards such as the greenhouse effect. Recycling construction materials such as ceramic waste and

* Corresponding author: aluko1977@graduate.utm.my

http://dx.doi.org/10.28991/CEJ-2023-09-04-014

aluminium fibres in concrete production will relieve the environment of this enormous waste and the hazards caused by pollution. Research on the reuse of construction waste has received massive attention due to its prospect of reducing construction costs and improving environmental benefits such as reducing CO_2 emissions into the atmosphere. Ferroconcrete, an emerging type of concrete, could be described as reinforced concrete consisting of galvanised iron mesh, cement, sand, stone, and water. The galvanised iron meshes are separated by layers and infused with concrete. Ferrocement differs from ferroconcrete because ferrocement uses mortar mix in its mesh layers, while ferroconcrete uses concrete mix in each of its mesh layers [1].

One of the major reasons for concrete cracks is the materials' thermal mismatch. It has been established that including short, closely spaced, and uniformly dispersed fibres in concrete would serve as a crack arrester and substantially improve its static and dynamic properties. Moreover, reinforced concrete is a composite material, where the reinforcement functions as the strengthening fibre and the concrete as the matrix. Thus, adding fibres makes the steel materials' performance comparable during thermal stress activities to lessen the deformational variance of concrete and reinforcing bars. However, it becomes impossible for fibre to entirely replace the moment-resisting steel reinforcement or upturn the concrete's flexural strength [2]. Therefore, the incorporation of fibres mainly serves as secondary reinforcement in concrete.

Supplementary Cementitious Materials (SCMs) have established emerging research opportunities in sustainable concrete development. Previous studies have revealed that the various applications of Ceramic Waste Powder (CWP) in concrete as a supplementary material have greatly improved the mechanical properties of concrete. The mechanical properties of ferrocement slabs using partial cement replacement by ceramic powder were studied by Dhilip Kumar et al. [3]. They found that the panel with a 10% replacement of ceramic powder offered more noticeable results than the other panels. Kannan et al. [4] carried out a study on CWP as cement replacement in mix proportions of 10% to 40% and observed that ceramic waste powder enhanced the mechanical properties with 20% of CWP cement replacement. Also, in self-compacting concrete, Subasi et al. [5] studied the addition of CWP as filler material in the amounts of 5%, 10%, 15%, and 20% (by weight). They observed that 15% replacement could be used as filler in self-compacting concretes if the strength and flowability properties are assessed together. A similar result was reported by Rawat et al. [6]. Also, Steiner et al. [7] studied the potential of ceramic tile polishing residues as SCMs in mortars, with mix proportions of 0%, 10%, 20%, 25%, 30%, and 40% mass fractions of cement. The results revealed that 30% is an optimum replacement for high efficiency. Also, Jackiewicz-Rek et al. [8] investigated the properties of cement mortars reformed with ceramic waste fillers, substituted with 10, 15, and 20% of ceramic fillers by cement weight. It was found that 20% replacement of fine aggregate with sanitary ceramic fillers enhanced compressive and flexural strength and reduced shrinkage.

Moreover, Awoyera et al. [9] researched the appropriateness of mortars prepared with laterite and CWP for mechanical properties assessment. The mortar specimen with 10% CW and 100% ceramic aggregate as a substitute for cement and sand offered higher strength values than other mixes and control specimens. It was attributed to a greater amount of ettringite, portlandite, and calcite than the control, which might be the reason for the strength gained. Rawat et al. [6] researched CWP as SCM in concrete by partially substituting cement with 5, 10, 15, and 20% CW. The mortar showed pozzolanic activity with up to 20% cement replacement and improved mechanical properties with 15% replacement. Apart from strength improvements, incorporating CWP improved fire resistance [10]. El-Gamal et al. [11] studied CWP as an effective SCM for high-temperature aversion. The strength characteristics of hardened Portland cement paste with 5, 10, and 20 CW (mass %), 5-10% CW provided effective thermal resistance, as reported. Also, ceramic sanitary ware was used as an aggregate replacement in concrete for high-temperature resistance [12]. The CWP, as a pozzolan admixture, has been found to contain metallic oxides such as Al_2O_3 and SiO_2, which can act as an effective partial replacement for cement to increase its mechanical properties. However, its usage creates a shortfall that increases water usage and difficulty in handling and placing the concrete mixture, but plasticiser can help reduce this limitation. Xuyong et al. [13] found that the sustainable use of ceramic waste as an SCM can significantly reduce the cost, thermal energy consumption, and carbon dioxide emissions of concrete.

Similarly, Rajaraman [14] studied the structural behaviour of aluminium fibres in concrete by replacing different percentages of cement with aluminium fibres in ratios of 0%, 0.8%, 1.0%, and 1.2%. The aluminium fibres used in the research study were looped at their ends to enhance their bond strength with the concrete. The results depict an enhancement in the compressive strength of concrete with a 1.2% optimum aluminium fibre fraction compared to conventional concrete. Sabapathy & Sabarish [15] investigated the strength characteristics of end-looped aluminium fibres in reinforced concrete. Three grades of concrete and five varying fibre substituting proportions (0, 0.5, 1, 1.5, and 2%) were applied in the study. Adding aluminium fibres to the composite enhanced the splitting tensile strength. The strength improved with an increasing fibre volume fraction. The splitting tensile strength ranged from 17.87% to 36.88% higher for the fractions from 0.5% to 2% for the M20 grade of concrete. Muwashee et al. [16] studied the characteristics of concrete and mortar strengthened with aluminium waste strips. The aluminium strip made from Coca-Cola was used due to its low density, ductility, and excellent tensile strength (about 310 MPa). The compressive and flexural strengths of aluminium strip concrete improved by 22% and 70%, respectively, when blended with 2.5% aluminium strip, as observed from the results. All these studies showed the impact waste aluminium fibres could have on the strength properties of eco-sustainable concrete.

Including fibre in the concrete mix has been beneficial in restraining plastic drying shrinkage cracking, improving concrete toughness, ductility, and tensile strength, and impairing crack progression. Some fibres efficiently provide greater bearing and resist shattering in concrete. Generally, fibre type, diameter, length, volume fraction, and aspect ratio affect fibre behaviour in concrete, while fibre volume and orientation affect the creep performance of rebars/tendons. Rita et al. [17] explored the properties of fibre-reinforced concrete in deferring crack creation during concrete setting. Research on the performance of fibre-reinforced concrete has been massive since a couple of decades ago. The fibres usable in concrete mixes consist of glass, metallic, synthetic (polyethene, polypropylene, polyvinyl alcohol, polyester), and natural (mineral, animal, and plant) fibres [18]. Besides the anti-cracking operation of fibre in concrete, it also provides reinforcing and toughening ('bridging effect') capabilities [19]. Lightweight materials have been identified as effective replacement components in concrete to decrease the overall weight of the material. Aluminium fibres in concrete possess low density and, therefore, low weight, superior malleability, easy machining, excellent corrosion resistance, and good thermal and electrical conductivity. Aluminium is also very easy to recycle and has average tensile strength. Aluminium fibres looped at their ends have been found to increase bond strength, but randomly dispersing these fibres can create a concentration of fibres in a section other than wholesome. This limitation can be improved with the concrete having equal layers of separation. Pakravan et al. [18] researched the mechanical behaviour of concrete reinforced with waste aluminium strips. Six batches of soft tin can fibres were cast with the addition of fibres in volumetric fractions of 0, 1, 2, 3, 4%, and 5%. The results show that the mechanical properties of concrete, such as the split tensile strength and flexural strength, improved with increasing fibre volume fractions up to 4%; beyond 4%, the strength begins to fall.

Design of experiments (DoE) has been a common technique gleaned from the statistical exploration of outcomes required to guarantee that well-founded results are obtained with little resources, time, and labour [20, 21]. It helps make an empirical model with appropriate considerations and conforming responses, limiting experiment numbers, and testing the parameter interrelationships [22]. Therefore, Response Surface Methodology (RSM) is a mathematical and statistical technique for evaluating a process in which the response of interest is affected by various variables [23]. The method aims to optimise the response, with parameters that affect the process as independent variables, while the response is called dependent variables. The RSM studies a suitable approximation relationship between input and output variables and detects the best operational environments for an investigated system or a region of the factor field that pleases the operating requirements. This research optimised and predicted the response of two variables, aluminium fibre and ceramic powder, on the effect of fibre-reinforced ferroconcrete. Analysing the compressive strength of ceramic waste-based concrete using an experiment and artificial neural network (ANN) approach was studied by Akhtar et al. [25]. The research concluded that ceramic powder's 10% and 20% replacement levels were optimum for increased compressive strength. The linear coefficient correlation (R^2) value indicated better model performance using statistical checks such as mean square and root mean square error to check its precision.

Incorporating SCMs in fibre-reinforced concrete for a sustainable solution has been extensively studied [24–26]. Over the past decade, significant contributions have been made to the study of ferrocement. However, extensive research has not been done on ferroconcrete and constituent additions of SCMs to improve their performance. Although Manasa et al. [27] researched the experimental studies of the behaviour of ferroconcrete beams, the compressive and flexural strengths were 16.32 and 13.62 N/mm^{2,} respectively, with a concrete mix of 1:3.

This study utilises a blend of waste aluminium fibres, Ceramic Waste Powder (CWP) as a partial replacement in a sustainable ferroconcrete mix, optimised using an RSM-based model for prediction, which is still unavailable in the literature because this has been identified as a gap. Pozzolanic wall tiles and aluminium fibres have been identified as significant sources of waste from construction, demolition, and reconstruction projects deposited in landfills, constituting a major health risk due to pollution and environmental degradation. Also, construction and housing development are thriving in many developing countries, particularly Nigeria. This research focuses on the sustainable and optimised use of these wastes by applying RSM. It presents a performance assessment of fibre-reinforced ferroconcrete for sustainable construction, with characterisation, optimisation and assessment of fibrous ferroconcrete mechanical characteristics containing CWP and aluminum in a laboratory experiment, using RSM for prediction and the model's performance evaluation. Engineers and construction stakeholders would find this a solution to shrinkage and cracking problems in concrete, benefiting low-embodied SCM as an eco-sustainable and tougher construction material.

2. Experimental study

2.1. Flowchart Methodology

The Flowchart Methodology of this research is available in Figure 1.

2.2. Materials

This section describes the sources, types, standards of material, and components in fibre-reinforced ferroconcrete.

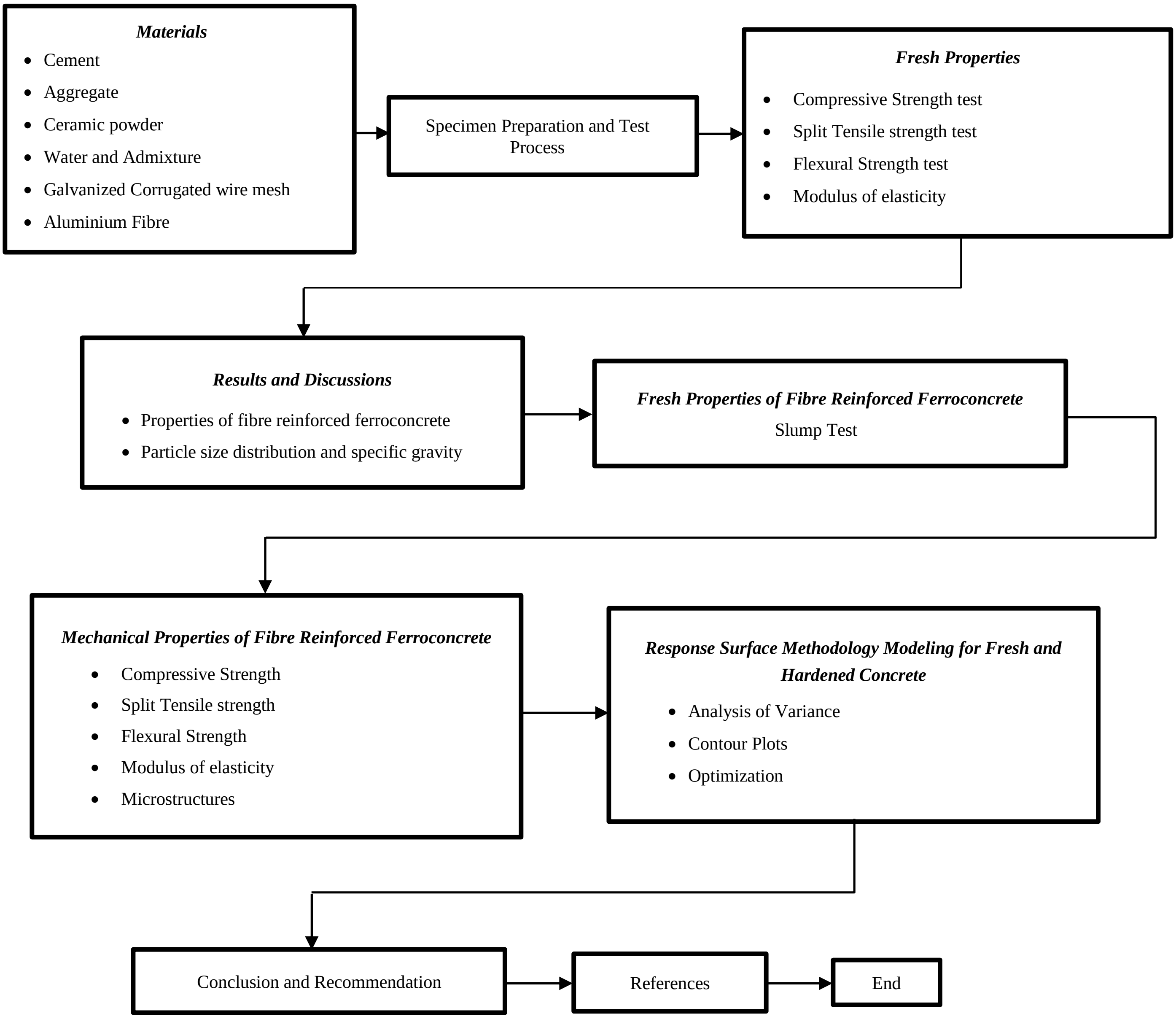

Figure 1. Flowchart of the methodology

2.2.1. Cement

Dangote 3X, Grade 42.5R Portland Cement, obtained from a cement shop in Ado Ekiti, Nigeria, was used in the study. The 3X stands for Xtra Strength, Xtra life, and Xtra Yield. Table 1 shows the mineral percentage composition of Dangote 3X Portland cement. Dangote Cement has so many properties; thus, the Al_2O_3 of about one percent composition corresponded slightly with type IV of ASTM [28]. The MgO and SiO_2 values are of Type I of ASTM [28], and the CaO and SO_3 percentage compositions are of Type IV of ASTM [28]. It has the highest uncombined lime, resulting in its low CaO. The cement conformed to BS EN 197-1.

Table 1. Mineral percentage composition of dangote 3X Portland cement

C_3S	C_2S	C_3A	C_4AF	Total Sum
33.33	26.47	14.33	4.77	78.9

2.2.2. Aggregates

River sand was sourced from a riverbank in Ado Ekiti, Nigeria, for fine aggregates, and tests were conducted following BS EN 12620 [29]. The fine aggregate is dark brown, with a specific gravity of 2.65 and a fine modulus of 2.35. Also, crushed granite stone aggregates of a maximum size of 5–10 mm were obtained from proposed construction sites within the main campus of Afe Babalola University, Ado Ekiti, Nigeria. Tests were conducted following BS EN 12620 [29]. The coarse aggregate's specific gravity and fine modulus are 2.73 and 3.62, respectively.

2.2.3. Ceramic Powder

The ceramic powder was obtained from the crushing of wall tiles. Pozzolanic wall tiles were obtained from construction sites within the main campus of the Federal Polytechnic, Ado Ekiti, Nigeria. Table 2 shows the chemical composition of ceramic waste, and the test conducted followed BS EN 12620 [29]. The ceramic powder had an ivory colour, Specific gravity of 2.46, and a fine modulus of 1.22, respectively.

Table 2. Chemical ccomposition of ceramic powder

Chemical oxide	Al_2O_3	ZrO_2	BaO	$(NaK)O_2$	SiO_2
Test result (%)	50	0	7.79	2.65	39.25

2.2.4. Water and High-Range Water Reducing Admixture

As per BS EN 206 [30] recommendations, clean water was used to mix concrete. The workability of the concrete was enhanced using a plasticiser. The brand of HRWRA used was COSTAMIX 200, obtained from Costar Building Product System in Ikeja, Lagos. Table 3 shows the properties of COSTAMIX 200.

Table 3. Properties of Costamix 200

Properties	Appearance	Chloride content	pH Value	Density	Air Entrainment	Water Reduction
Range	Brown low viscous liquid	Nil	7-9	$1.18 g/cm^3 + 0.01$	<2%	20-30%

2.2.5. Galvanized Corrugated Wire Mesh

Rolls of Wire mesh of steel material with internal cell dimensions of 25 mm×15 mm were purchased from a wire mesh store in Ado, Nigeria, and it is shown in Figure 2-a.

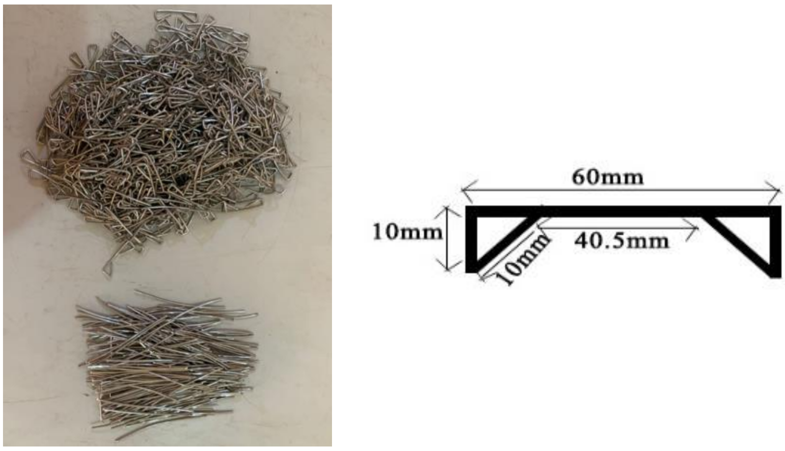

(a) (b)

Figure 2. a) Aluminum fibres, b) Graphical representation of looped Aluminium fibre

2.2.6 Aluminium Fibre

Aluminium fibres were obtained from an external layer of armoured cables. Fibres measuring 100 mm in length and 2.0mm in diameter were looped at their ends with lengths of 10 mm, each shrinking the total length of the fibre to 60 mm. Figures 2-a and 2-b show the physical picture and graphical representation of the aluminium fibre (aspect ratio = 50). The tensile stress of the aluminium fibre was 382 N which gave 121.57 N/mm^2 as the tensile strength. Also, Galvanized Corrugated Steel-Wire Mesh Rolls with internal cell dimensions of 25 mm × 15 mm were purchased from a wire mesh store in Ado-Ekiti, Nigeria.

2.3. RSM Model Development

The RSM is usually characterised by a quadratic model expressed in a second-order equation, as presented in equation 1. The independent variables considered in the study are aluminium fibre and ceramic powder, which varied between 0, 1%, 2%, 0, 10%, and 20%, respectively. In all, thirteen experimental runs were created by Design-Expert software 11.01 using the Central Composite Design (CCD) response surface methodology for M15-grade concrete. The total number of the CCD experiment is 2k + 2k + n, where k is the number of independent variables and n is the number of the centre point [31]. Table 4 presents all experimental points to be considered in their actual terms:

$$y = a_0 + \sum_{i=1}^{2} a_i x_1 + \sum_{i=1}^{2} a_{ij} x_i x_j \tag{1}$$

Where y is the forecasted value, a_0 is a constant and a_i and a_{ij} are the regression coefficients of the RSM model. The x_i and x_j are the factor variables. The statistical parameters to be used in the regression analysis of the RSM model are the coefficient of correlation (R), coefficient of determination (R^2), and adequate prediction.

Table 4. Experimental design points

Test No	1	2	3	4	5	6	7	8	9	10	11	12	13
Ceramic (%)	10	10	10	20	10	0	20	10	0	0	10	10	20
Fibre (%)	1	1	0	0	1	0	2	2	1	2	1	1	1

Here, x is the real value, and y is the forecasted value. $\overline{x}$ and $\overline{y}$ were the average forecasted and real values, respectively, and n is the number of samples. The factor codes signifying the low, centre, and high points of the variables in the RSM model are shown in Table 5.

Table 5. Factor and factor level for RSM

Factor	Code	Factors level of code		
		Low level	Intermediate level	High level
Aluminium Fibre (%)	A	0	1	2
Ceramic powder (%)	B	0	10	20

2.4. Specimen Preparation and Test Process

The material for samples of the fibre-reinforced concrete was mixed in a mixing pan of concrete capacity with a weight of 68 kg. Table 6 presents the mix proportions for the constituent materials. Firstly, the measured quantity of cement and ceramic powder was thoroughly mixed, followed closely by fine and coarse aggregate quantities. 80% of the water was mixed with the required superplasticiser dosage and poured into the mixing pan. Mixing thoroughly took about 4 minutes; half quantities of aluminium fibres were randomly dispersed in the mixing pan, and mixing continued for another 1 minute. Finally, the other half of the fibres were dispersed again in the mixing pan, and mixing continued until a homogenous concrete was achieved, as shown in Figure 2. After mixing, the concrete was placed in the mould with layers of separation of 20 mm. Three layers of separation were used for the cubes and beams, where each layer of separation had a corrugated wire mesh with an intermediary distance of 20 mm. For the cylindrical layer, just one layer of a cylindrical mesh was used. The sizes of the mesh layer for the cube were 80 mm × 80 mm × 80 mm, for the beam, 80 mm × 480 mm, and for the cylindrical, a mesh of 75 mm in diameter. With each layer, a hand trowel was used for the effective distribution and compaction of the concrete. The samples were kept at room temperature, de-moulded, and cured for 28 days before testing.

Table 6. Mix proportion for constituent materials

Test No	Aluminium Fibre (%)	Ceramic powder (%)	Cement (kg/m^3)	Fine Aggregate (kg/m^3)	Coarse Aggregate (kg/m^3)	Water (kg/m^3)	Super Plasticizer (kg/m^3)
1	1	10	540	800	1000	180	15
2	1	10	540	800	1000	180	15
3	0	10	540	800	1000	180	15
4	0	20	480	800	1000	180	15
5	1	10	540	800	1000	180	15
6	0	0	600	800	1000	180	15
7	2	20	480	800	1000	180	15
8	2	10	540	800	1000	180	15
9	1	0	600	800	1000	180	15
10	2	0	600	800	1000	180	15
11	1	10	540	800	1000	180	15
12	1	10	540	800	1000	180	15
13	1	20	480	800	1000	180	15

2.5. Fresh Properties

Fresh fibre-reinforced ferroconcrete and hardened samples for curing are shown in Figures 3-a and 3-b. The consistency of the fresh ferroconcrete was assessed through a slump test, conforming to BS EN 12350-2 [32]. A cone of an upper diameter of 100 mm, lower diameter of 200 mm, and height of 300 mm was used to carry out the test. The cone was firmly placed on a horizontal surface and filled in three layers of concrete, with each layer tamped 25 times. Once the cone got filled, the overflowing concrete was removed, and the cone was lifted vertically and placed upside down next to the concrete. The slump level was measured from the tamping rod down to the top of the slump of the concrete.

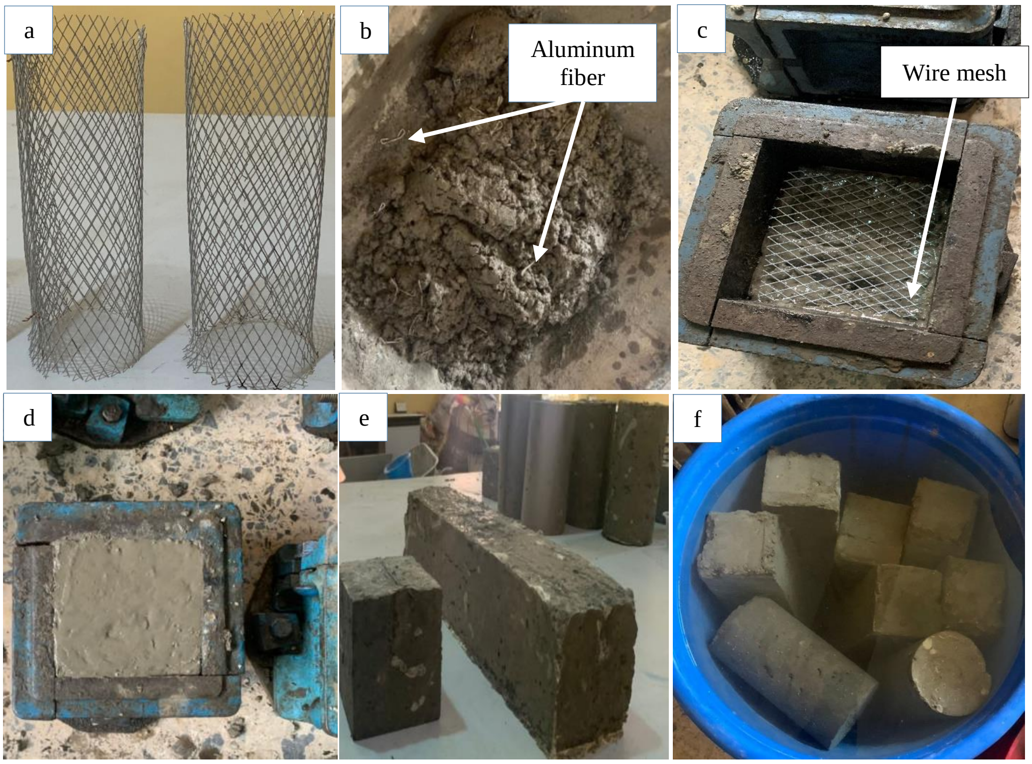

Figure 3. a) Wire mesh, b) Fresh fibre-reinforced ferroconcrete, c) Wire mesh in cube casting, d) Cast cube, e) de-moulded samples for curing, f) Samples in curing container

2.6. Compressive Strength Test

The compressive strengths assessment was obtained according to ASTM C349-08 [33] using an ELE compression machine having a crushing capacity of over 2000 kN on 100 mm cube specimens. The test results were the average of three measurements obtained from three cube specimens and calculated with Equation 1.

$$f_c = \frac{L}{A} \tag{1}$$

where; fc is the strength (N/mm^2), L is load (N), and A is the cross-sectional area (mm^2).

2.7. Split Tensile Strength Test

Cylindrical samples of 100 mm diameter and 200 mm height were tested using a compression testing machine following BS EN 12390-6 [34]. The maximum loads when the sample split was recorded, and the split tensile strength of the sample was determined with Equation 2.

$$ft = \frac{2P}{(\pi \text{ DL})} \tag{2}$$

where; f_t is Split tensile Strength (N/mm^2), P is Load at failure (N), L is the Length of the cylinder (mm), and D is the diameter of the cylinder (mm).

2.8. Flexural Strength Test

A three-point test in conformity with ASTM C348 [35] was used to perform the test at 28 days to determine flexural strength. A centerline was marked at the top of the (100×100×500) mm prism specimens. The specimens were tested under a central line load while simply supported, 400 mm. This test was carried out using a universal test machine with a load capacity of 100kN. The following expression is used for the estimation of flexural strength.

$$f_s = \frac{3PL}{2BD2} \tag{3}$$

where, f_s is flexural strength (N/mm^2), P is max load (kN), L is Effective Length (mm), B is Width (mm), D is Depth (mm).

2.9. Modulus of Elasticity

Density affects the calculating theory and mathematical concrete modulus of elasticity, following ACI-318-14-report, 2014 [36] section 8.5. The modulus of elasticity is given as:

$$Ec = 4700\sqrt{f_c'} \tag{4}$$

where; f'_c is compressive strength in N/mm^2. This formula is valid for normal-weight concrete having a density between 1440 and 2560 kg/m^3.

3. Results and Discussion

Test results were obtained from fibre-reinforced ferroconcrete's fresh and hardened properties were discussed. The experimental program for the research had thirteen runs which included varying the proportion of ceramic powder and aluminium fibre. Their mechanical properties were tested for compressive, flexural, and split tensile strength tests after 28-day water curing. RSM model was adopted to predict the outcome of the proportioning of variables (ceramic powder and aluminium fibre) impact on the mechanical characteristics of the fibre-reinforced ferroconcrete. The significance of the RSM models was evaluated based on statistical parameters like the coefficient of determination (R^2).

3.1. Properties of Fibre-Reinforced Ferroconcrete

The properties of constituent material notably influenced the fresh and hardened characteristics of fibre-reinforced ferroconcrete. Thus, the need to obtain the test result undertaken on fresh and hardened properties of the ferroconcrete.

3.1.1. Particle Size Distribution and Specific Gravity

Figure 4 shows the sieve analysis results for ceramic powder, fine aggregate, and coarse aggregate. The uniformity coefficient Cu for ceramic powder, fine aggregate, and coarse aggregate are given respectively as 2.07, 1.33, and 1.42, while the coefficient of gradation Cc is given as 0.506, 1.76, and 0.96, respectively. The specific gravity for fine aggregate and ceramic powder is 2.65 and 2.46, respectively. The diameter in the particle size distribution curve corresponding to 10% finer is called the effective size of D_{10}, while the diameter corresponding to 60% and 30% finer is called effective sizes D_{60} and D_{30}.

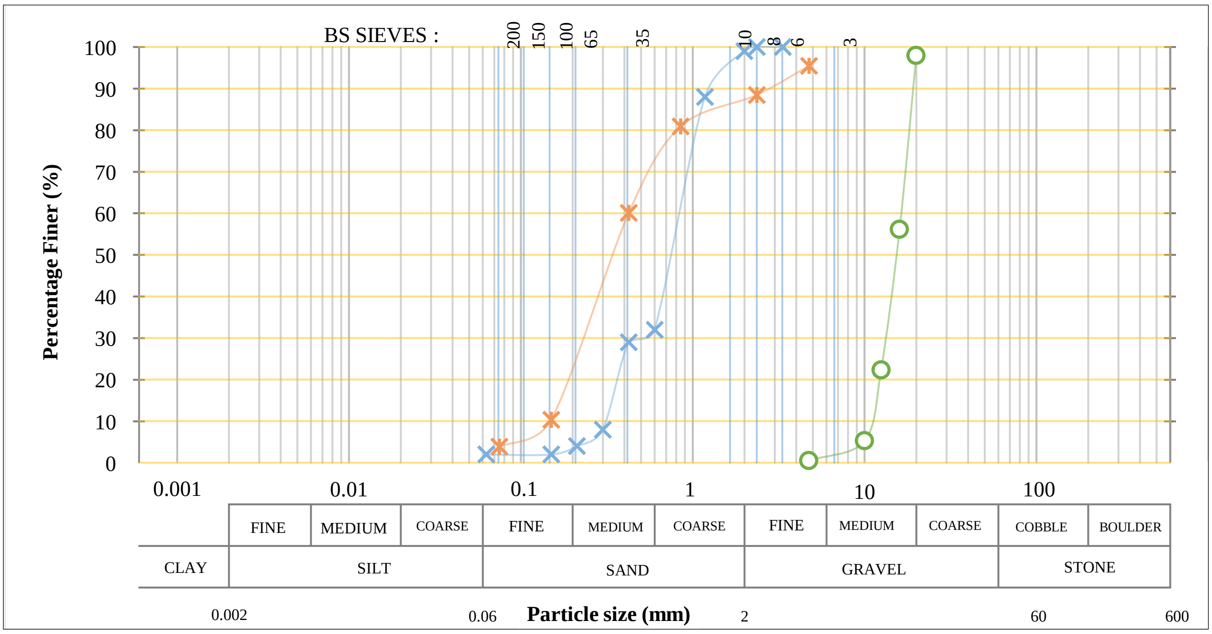

Figure 4. Sieve analysis distribution curve of ceramic powder (blue), fine aggregate (orange), coarse aggregate (green)

3.1.2. Fresh Properties of Fibre Reinforced Ferro Concrete

1.1.2.1. Slump Test

Table 7 shows the mixing proportions and their varying slumps. The table shows that the fibre-reinforced ferroconcrete has a low workability slump flow according to BS EN 12350-2 [37]. Run 1 shows that the control specimen, which contained 0% fibre and 0% ceramic powder, had the highest slump with a value of 40 mm as compared with run 3, which, with the replacement of cement with 10% ceramic powder and the addition of 1% aluminium fibre, had a slump value of 35 mm. This shows that run 3 had decreased workability and consistency. As the percentage of ceramic powder increased, we saw the workability further reduce to 30mm, as seen in run 5. This further indicates that the higher the percentage of ceramic powder, the higher the water demand for better workability. This result is consistent with Cheng et al. [38], who reported that the relatively higher values of Ceramic Waste Powder compared with cement increased the water demand and resulted in lower slump flow values. Also, run 11 contains 10% ceramic powder and 2% aluminium fibre with a slump value of 19 mm. The presence of aluminium fibre in the concrete mix contributes to the slump reduction because the slump gradually decreased as increments in the proportions of aluminium fibres were added. This is in agreement with Zeyad [39], who reported that slump flow decreased appreciably when hooked-end steel, mild steel, carved steel basalt rock, and polypropylene fibres were added to the concrete. Kanag et al. [40] also reported drastic workability reduction of the concrete at higher fibre dosages to such a great extent that even admixtures may not help reduce the damage. The CWP and aluminium fibre combination significantly reduced the ferroconcrete's workability from 40mm with the control specimen to 18 mm, as seen in Run 13. For this study, the slump (mm) was plotted as a function of the different experimental runs (Figure 5).

Table 7. Result of Experimental run with their corresponding slump (mm)

Test	1	2	3	4	5	6	7	8	9	10	11	12	13
Ceramic proportion (%)	0	0	10	0	20	10	10	10	10	10	10	20	20
Aluminium Fibre (%)	0	1	0	2	0	1	1	1	1	1	2	1	2
Slump (mm)	40	29	35	20	30	28	25	28	25	24	19	27	18

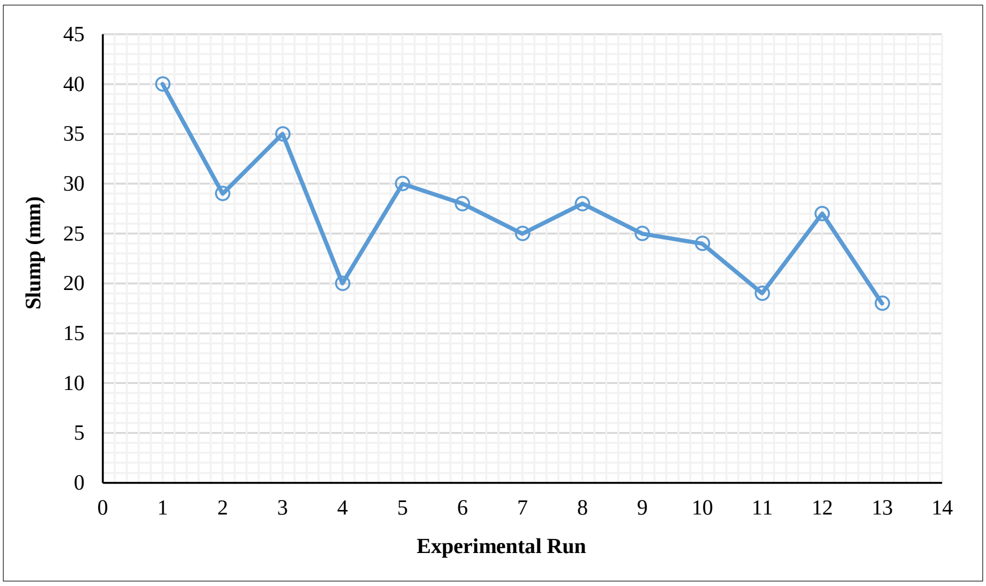

Figure 5. Effects of aluminium fibre added in proportions of 0%, 1%, and 2% and ceramic powder in proportions of 0%, 10%, and 20% on the slump properties of fibre-reinforced ferroconcrete

3.2. Mechanical Properties of Fibre-Reinforced Ferroconcrete

Concrete cubes, prisms, and cylinders were tested for compressive, flexural, and split tensile strength. Table 8 shows the summarised result of the individual strengths corresponding to the mixed proportions. Also, Figure 6 shows the combination of compressive, flexural, and split tensile strength results plotted as a function of the experimental run.

Table 8. Combined results of compressive strength, flexural strength, and split tensile strength

Test	Age Days	Mix Proportion of Ceramic powder (%)	Mix Proportion of Fibre (%)	Compressive Strength (N/mm^2)	Flexural Strength (N/mm^2)	Split Tensile Strength (N/mm^2)
1	28	0.000	0.000	13.060	5.720	3.110
2	28	0.000	1.000	14.190	5.980	3.350
3	28	10.000	0.000	12.930	5.090	2.720
4	28	0.000	2.000	13.850	6.130	3.260
5	28	20.000	0.000	14.670	5.660	2.910
6	28	10.000	1.000	13.560	5.290	2.840
7	28	10.000	1.000	13.110	5.460	2.890
8	28	10.000	1.000	12.890	5.380	2.760
9	28	10.000	1.000	13.220	5.510	2.850
10	28	10.000	1.000	13.180	5.270	2.890
11	28	10.000	2.000	11.960	6.190	2.790
12	28	20.000	1.000	15.880	6.680	3.830
13	28	20.000	2.000	15.130	6.940	3.570

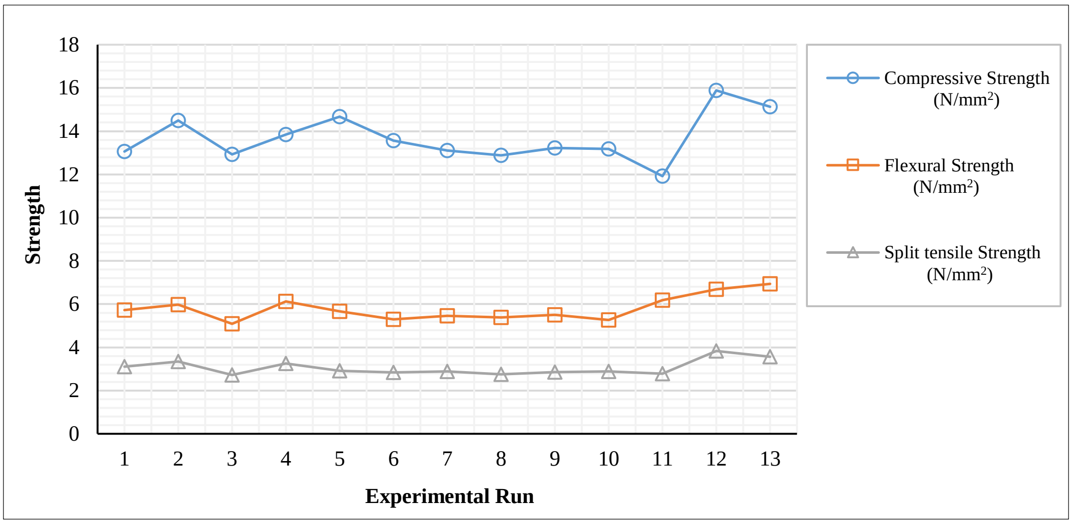

Figure 6. Effects of aluminium fibre added in proportions of 0%, 1%, and 2% and ceramic powder in proportions of 0%, 10%, and 20% on the compressive strength, flexural strength, and split tensile strength of fibre-reinforced ferroconcrete

3.2.1. Compressive Strength

The compressive strength of the fibre-reinforced concrete was plotted as a function of different experimental runs, as shown in Figure 5. It was observed from the experimental testing that the concrete cube specimens did not entirely rupture when impacted with loads because of the layers of wire mesh. Kiran & Rao [41] reported that the compressive strength test on ferroconcrete beams did not entirely rupture on failure due to the wire mesh. The lowest compressive strength of 11.96 N/mm^2 was observed at run 11, which contained 2% fibre and 10% ceramic powder. Run 2 had a strength of 14.19 N/mm^2 and contained 1% fibre and 0% ceramic powder, while run 4 had a strength of 13.85 N/mm^2 with 0% ceramic powder and 2% aluminium fibre, and this shows that the addition of more fibres reduces compressive strength. This is consistent with the compressive strength result of Datye & Pawar [42], who researched aluminium fibre matrix in concrete. They found that an increase in compressive strength was observed for up to 7.5% addition of aluminium fibre matrix to the concrete with a strength of 22.2 N/mm^2; with further addition of 10% fibres to the concrete, compressive strength reduced to 21.7 N/mm^2.The reference mix for ferroconcrete had a strength of 13.06 N/mm^2, while run 12 had the highest compressive strength of 15.88 N/mm^2, containing 20% CWP and 1% aluminium fibre. The various experimental runs suggest that increasing ceramic powder up to 20% will yield increased compressive strength; however, proportions of more than 1% of aluminium fibre will ultimately reduce the strength. On average, the compressive strength was poor, possibly due to the pore spaces in the concrete and fibres sharing part of the cement paste meant to hold the aggregates, making CSH formation insufficient as the hydration progresses. The compressive strength results show that the concrete is an M15 grade. Zhang et al. [19] report that variation in the compressive strength of concrete containing fibres can be explained by the air trapped around the fibres contributing to the reduced strength. This supposition is based on the fact that adding fibres reduces the efficiency of the fresh concrete properties compared with non-fibrous concrete.

3.2.2. Split Tensile Strength

The split tensile strength of the fibre-reinforced ferroconcrete as a function of different experimental runs is shown in Figure 5. The test result showed that after being loaded up to failure, the specimen did not split into halves because the intermediary wire mesh layer provided post-cracking stress redistribution [43–45] and bridging capabilities. This agrees with Manasa et al. [27], who report that the ferroconcrete beams used in their experiment did not split into halves upon failure. The lowest split tensile strength was 2.72 N/mm^2, containing 10% ceramic powder and 0% fibre. A remarkable surge in strength was observed with 3.57 N/mm^{2,} which contained 20% ceramic powder and 2% fibre; however, the control mix decreased to 3.11 N/mm^2. The maximum split tensile strength was 3.83 N/mm^2, showing a remarkable 7.2% increase in flexural strength between samples containing 20% ceramic powder and 1% fibre and samples containing 20% ceramic powder and 2% fibre. Rawat et al. [6] studied the behaviour of mortar and concrete reinforced with aluminium strips, the results of the research show that the tensile strength is highly increased in concrete and mortars with aluminum strips , this can be attributed to two reasons, first, the high tensile strength of Aluminum strips which is 310 MPa, and secondly the action of the strips which gives extra bonds with concrete and make concrete more strong and reduce the propagation of cracks during loading, however our research with aluminium fibre used in the fibre reinforced ferroncrete shows a low tensile strength of 121.57 N/mm^2 which can be the reason for our reduced tensile strength but one deduction is consistent, both ferroconcrete with ceramic powder and aluminium fibre and aluminium strips on concrete do not rupture on failure which means the fibres provide more toughness to the concrete, this result is also consistent with Ravinder [46], who confirms this in the research on Strength characteristics of Coca-Cola tin waste as fibres in concrete. This implies that an increase in fibre by up to 1% and ceramic powder by up to 20% will increase the split tensile strength of the concrete specimen but will reduce it when the fibre proportion increases to 2%. A study by Kiran & Rao [41] confirms the efficacy of an optimum and higher fibre fraction on concrete strength improvement.

3.2.3. Flexural Strength

The prism specimens, after failure, did not split into halves but were held slightly by the wire mesh towards the bottom. Flexural strength was plotted as a function of the experimental run, as shown in Figure 5. A combination of 10% ceramic powder and 1% fibre gave the least flexural strength of 5.27 N/mm^2, which increased to 6.68 N/mm^2 with a percentage of 20% ceramic powder and 1% fibre. The maximum flexural strength was 6.94 N/mm^2, containing 20% ceramic powder and 2% fibre. This suggests that increased aluminium fibre and ceramic powder proportions will yield increased flexural strength. This result agrees with Ilya & Chea [47], who reported an increasing flexural strength value with a correspondingly increasing fibre in the concrete specimen. The normal concrete had a value of 0.922 N/mm^2. However, when the strength reaches its highest value at the specimen with 2% of fibre, which is 1.003 N/mm^2, the value decreases substantially at the specimen with 1% fibre, with a value of 0.224 N/mm^2. It can be deduced that the combination of ceramic powder and aluminium fibres at a higher percentage gives more ductility and flexural strength to the fibre-reinforced ferroconcrete. However, fibre-reinforced ferroconcrete shows a 2.7% increase in strength between 20% ceramic powder, 2% aluminium fibre and 20% ceramic powder and 1% fibre, while a surge in strength of up to 21.32% is observed between ferroconcrete containing 20% ceramic powder, 2% aluminium fibre and the control concrete.

3.2.4. Modulus of Elasticity

Table 9 Displays the density and corresponding modulus of elasticity with an increase in varying proportions of aluminium fibre and ceramic powder.

Table 9. Modulus of elasticity of fibre-reinforced ferroconcrete

Experimental Run	Proportion of Ceramic powder %	% of Aluminium fibre	Mass (kg)	Volume (m^3)	Density (kg/m^3)	Modulus of Elasticity *E*c (GPa)
1	0.000	0.000	2.324	0.001	2324	16.985
2	0.000	1.000	2.338	0.001	2338	17.890
3	10.000	0.000	2.341	0.001	2341	16.900
4	0.000	2.000	2.368	0.001	2368	17.491
5	20.000	0.000	2.248	0.001	2248	18.001
6	10.000	1.000	2.368	0.001	2368	17.307
7	10.000	1.000	2.352	0.001	2352	17.017
8	10.000	1.000	2.376	0.001	2376	16.874
9	10.000	1.000	2.389	0.001	2389	17.088
10	10.000	1.000	2.522	0.001	2522	17.063
11	10.000	2.000	2.378	0.001	2378	16.524
12	20.000	1.000	2.495	0.001	2495	18.729
13	20.000	2.000	2.442	0.001	2442	18.281

Increases in the concrete modulus of elasticity were synonymous with increases in concrete strength. The stiffer the material, the higher the modulus value. The same parameters affecting concrete compressive strength were also accountable for elastic modulus. The highest compressive strength of 15.88 N/mm^2 is observed at 20% ceramic powder and 1% aluminium fibre, corresponding to 18.729 GPa as the maximum modulus of elasticity for the ferroconcrete. Parida et al. [48] report the simultaneous improvement in the modulus of elasticity of steel fibre-reinforced concrete with the concrete's strength. It could be inferred that the steel fibres upturn the ultimate stress and the equivalent ultimate strain compared to the unreinforced concrete. This indicates that the concrete does not entirely break into pieces when loaded until failure and suffers breakage, showing good bonding between the steel and concrete and fibre bridging action [2, 49].

3.3. Response Surface Methodology Modelling for Fresh and Mechanical Properties

RSM models were adopted to analyse the effect of experimental data results on fibre-reinforced ferroconcrete. According to the Central composite design by the design expert software, the model was undertaken to examine the impact of the variables (Aluminium fibre and Ceramic Powder) and predict and optimise the fresh and mechanical properties of the ferroconcrete at 28 days. The experimental results were analysed to obtain the optimum combination of variables (Aluminium fibre and ceramic powder) on the slump, compressive strength, modulus of elasticity, flexural strength, and split tensile strength of the fibre-reinforced ferroconcrete. The regression models were obtained by fitting experimental data to linear, interactive, and quadratic terms. The adequacy of the model was checked using a model sum of squares and model summary statistics, and the results indicate p-values lower than 0.05. The final equation obtained regarding the coded factors is given in Equations 5 to 9.

$$f_s = 26.28 - 2.33A - 8.00B + 2.00AB + 1.03A^2 + 0.0345B^2 \quad (5)$$

$$f_{cs} = 13.23 + 0.7133A + 0.0400B - 0.0825AB + 1.88A^2 - 0.8831B^2 \quad (6)$$

$$f_{moe} = 17.11 + 0.4408A + 0.0683B - 0.0565AB + 1.11A^2 - 0.4844B^2 \quad (7)$$

$$f_{fs} = 5.45 + 0.2417A + 0.4650B - 0.2175AB + 0.7184A^2 - 0.0284B^2 \quad (8)$$

$$f_{sts} = 2.89 + 0.0983A + 0.1467B - 0.1275AB + 0.6057A^2 - 0.2293B^2 \quad (9)$$

where A is ceramic powder, and B is aluminium fibre.

3.3.1. The Analysis of Variance (ANOVA)

The suitability and fitness of the model were tested using the analysis of variance (ANOVA). The results indicate that the equation adequately represents the actual relationship between the input parameters and the desired responses, as shown in Table 10. The ANOVA was carried out to determine the contributions of the linear interaction and quadratic terms. The statistically significant terms were determined according to the student's t-test (p-value < 0.05). Terms with p-values less than 0.05 were judged significant, while those greater than 0.05 were insignificant. Table 10 shows the significance of the models achieved from ANOVA of the Fiber-reinforced ferroconcrete containing Ceramic Powder and Aluminium Powder, respectively. It shows that the model of the slump was most remarkable at a 95% confidence level, with an F-value of 27.64 and a p-value of 0.0002, having a lack of fit value of 0.5676, which was insignificant, indicating a satisfactory fit for the data.

Compressive strength was non-trivial at 95% confidence levels with an F value of 15.50, a p-value of 0.0011, and a lack of fit value of 0.0704. Flexural strength was notable at a 95% confidence level with an F-value of 19.43 and a p-value of 0.0006 with a lack of fit of 0.0508. Also, split tensile strength was significant at a 95% confidence level with an F-value of 10.70, a p-value of 0.0035, and a lack of fit of 0.0086. R^2 values of 0.9518, 0.9172, 0.9328, and 0.8843 corresponding to slump, compressive strength, flexural strength, and split tensile strength were satisfactory since they all tended to 1 and were greater than 0.8. Although LOF was significant for split tensile strength, however did not nullify the model for predictive purposes since R^2 was roughly 0.90. For a model to possess a good prediction capability, it must have a non-significant lack of fits [50]. These high values for R^2 imply that the regressors in the model explain approximately 90% of the overall modification of outcomes. [51], carried out an analysis comparing RSM and the hybrid training approach of artificial neural networks in modelling the properties of concrete containing steel fibre extracted from waste tires. The conclusion was that the RSM model's correlation coefficient (R) should be closer to 1. Schober & Schwarte [52] inferred that R values of more than 0.9 show an excellent correlation between the actual and predicted data in all developed RSM model scenarios, which were trained using actual data, and they predicted the responses efficiently.

Table 10. ANOVA for experimental results

Source	DF	Slump			Compressive Strength			MOE			Flexural Strength			Split Tensile Strength		
		SS	F value	P value	SS	F value	P value	SS	F value	P value	SS	F value	P value	SS	F value	P value
Model	5	436.22	27.64	0.0002	12.91	15.50	0.0011	4.64	18.90	0.0006	3.56	19.43	0.0006	1.27	10.70	0.0035
A	1	32.67	10.35	0.0147	3.05	18.32	0.0037	1.17	23.75	0.0018	0.3504	9.57	0.0175	0.0580	2.45	0.1613
B	1	384.00	121.67	0.0001	0.0096	0.0576	0.8172	0.0280	0.5707	0.4746	1.30	35.43	0.0006	0.1291	5.46	0.0521
AB	1	16.00	5.07	0.0591	0.0272	0.1634	0.6981	0.0128	0.2601	0.6257	0.1892	5.17	0.0572	0.0650	2.75	0.1412
A^2	1	2.96	0.9365	0.3654	9.73	58.40	0.0001	3.42	69.70	0.0001	1.43	38.94	0.0004	1.01	42.84	0.0003
B^2	1	0.0033	0.0010	0.9752	2.15	12.93	0.0088	0.648	13.20	0.0084	0.0022	0.0610	0.8119	0.1452	6.14	0.0423
Residual	7	22.09			1.17			0.3437			0.2563			0.1655		
Adeq. Prec.		17.7047			12.6697			13.9950			16.2131			10.7667		
Std. Dev.		1.78			0.4082			0.2216			0.1913			0.1538		
Mean		26.77			13.68			17.40			5.79			3.06		
R^2		0.9518			0.9172			0.9311			0.9328			0.8843		

SS: Sum of squares; DF: Degree of freedom; SD: standard deviation; MOE: Modulus of Elasticity; R^2: Coefficient of determination; AP: Adequate precision, A = Ceramic Powder; B = Aluminium Fibre.

3.3.2. Contour Plot

Contour plots are valuable for creating response data and an operating environment [21, 53]. A contour plot is the geometric illustration of a 3-D correlation to two extents, with X1 and X2 (independent variables) plotted on x- and y-scales and response values signified by contours (z-scale). The variables in this study were aluminium fibre and ceramic powder, where aluminium fibre is plotted as a function of ceramic powder, as shown in Figures 7-a to 7-j. Figures a and b represent the 2D contour plot and the 3D response of the slump flow, respectively; c and d for compressive strength; e and f for modulus of elasticity; g and h for flexural strength; and i and j for split tensile strength. Figure 7-a shows the contour plot of the slump flow, where the red zone in the bottom left corner represents the highest slump flow significance for control, marked at 40mm. The 3D response from Figure 7-b confirms this result with the red zone tilted to the top, which shows an increased slump and further tilts downwards as slump flow decreases with the simultaneous addition of aluminium fibres and ceramic powder. Figure 7-c contour plot shows that the peak strength is recorded at 20% ceramic powder and 1% aluminium fibre. This indicates that the quantity of fibre and ceramic powder increases by up to 1% and 20%, respectively. The compressive strength reaches its peak, which is displayed in the middle of the red zone at the right corner. With the addition of more fibres, the zones grow lighter and turn yellow, which signifies reduced strength. The 3D response, as shown in Figure 7-d, signifies the graph trend growing to the top at the middle, which indicates the highest compressive strength achieved; after that, it tilts downwards as indicated by the yellow zone, signifying reducing strength. Figure 7-e shows the same properties as the modulus of elasticity. An increase in aluminium fibre up to 1% and an increase in ceramic powder up to 20% resulted in a higher modulus of elasticity but decreased when aluminium fibre increased more than 1%. Also, Figure 7-g contour plot clearly shows that as ceramic powder and aluminium fibre increase simultaneously, the flexural strength will give maximum strength close to 7 N/mm^2. The red zones at the top right section signify peak strengths at the various percentages of the two-factor variables. Figure 7-i shows a similar effect as Figure 7-a, with peak split tensile strength recorded at 20% ceramic powder and 1% aluminium fibre and a steady decrease as the percentage of aluminium fibre increases.

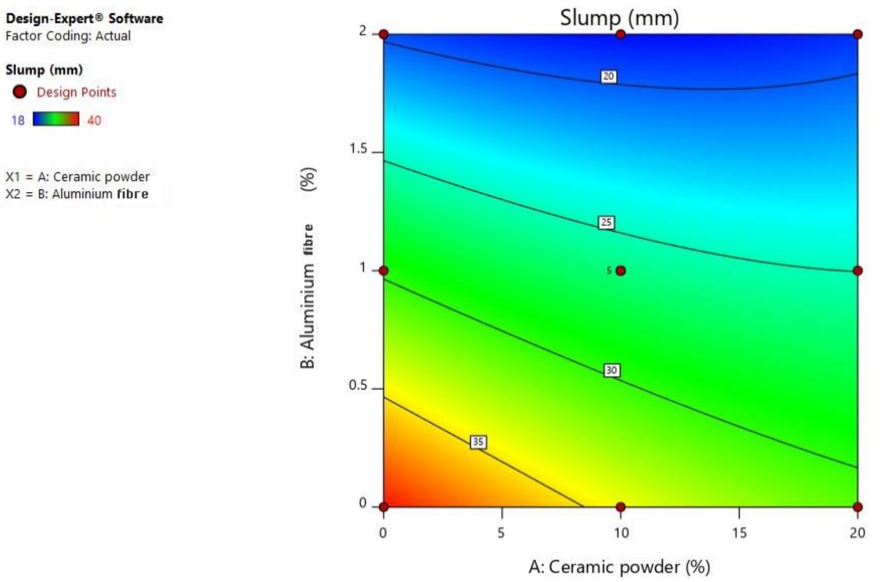

(a)

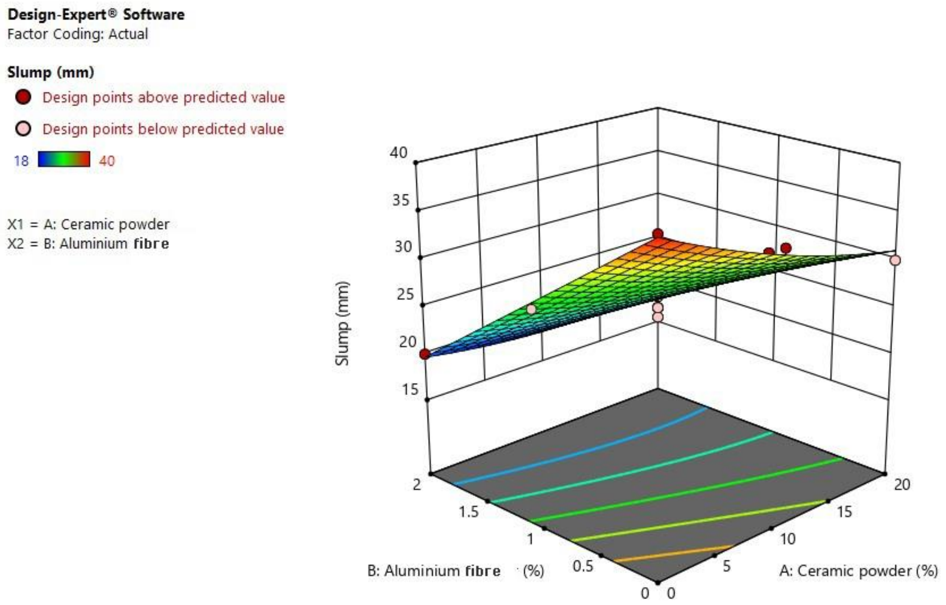
Design-Expert® Software
Factor Coding: Actual
Slump (mm)
Design points above predicted value
Design points below predicted value
18
40
X1 = A: Ceramic powder
X2 = B: Aluminium fibre
Slump (mm)
B: Aluminium fibre (%)
A: Ceramic powder (%)

(b)

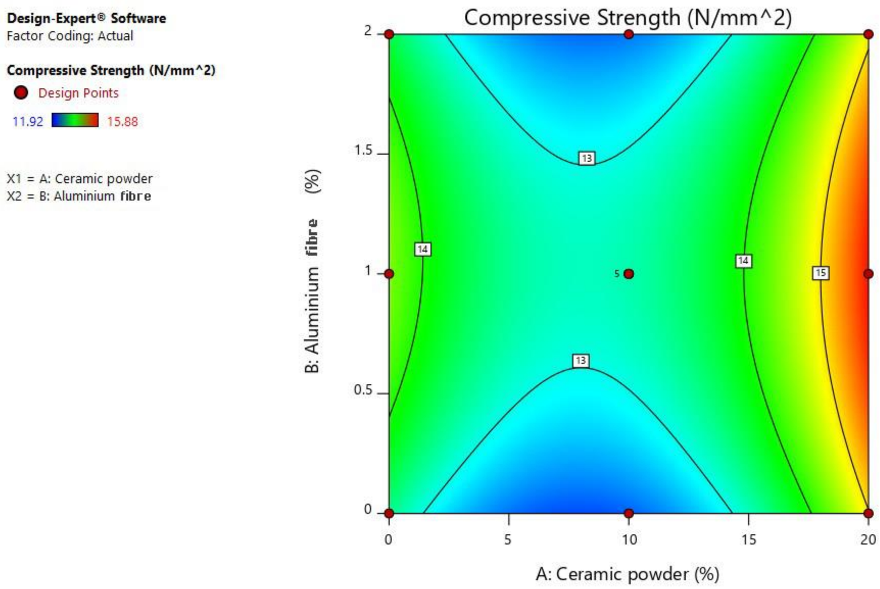
Design-Expert® Software
Factor Coding: Actual
Compressive Strength (N/mm^2)
Design Points
11.92
15.88
X1 = A: Ceramic powder
X2 = B: Aluminium fibre
Compressive Strength (N/mm^2)
B: Aluminium fibre (%)
A: Ceramic powder (%)

(c)

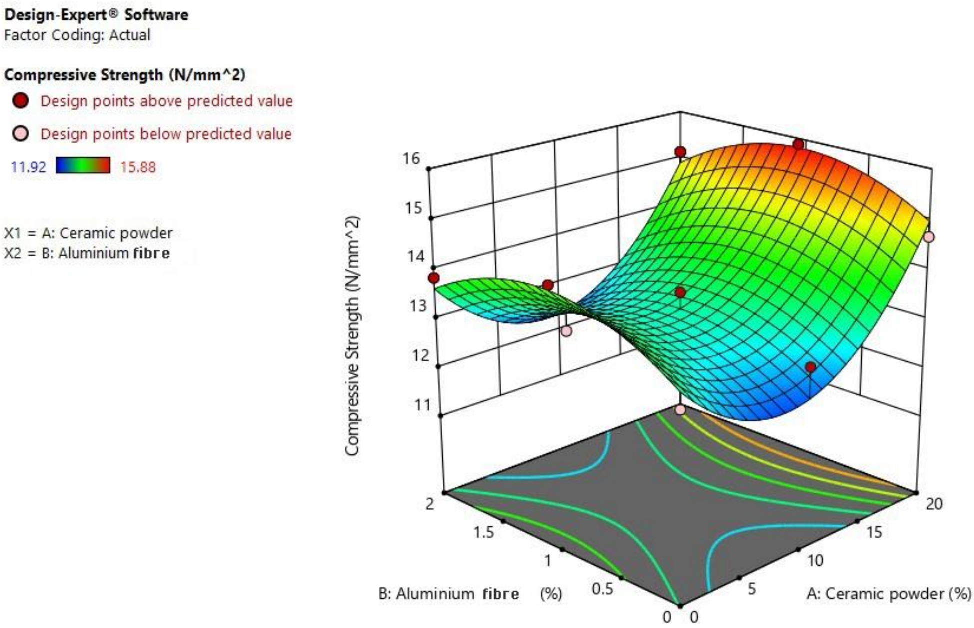
Design-Expert® Software
Factor Coding: Actual
Compressive Strength (N/mm^2)
Design points above predicted value
Design points below predicted value
11.92
15.88
X1 = A: Ceramic powder
X2 = B: Aluminium fibre
Compressive Strength (N/mm^2)
B: Aluminium fibre (%)
A: Ceramic powder (%)

(d)

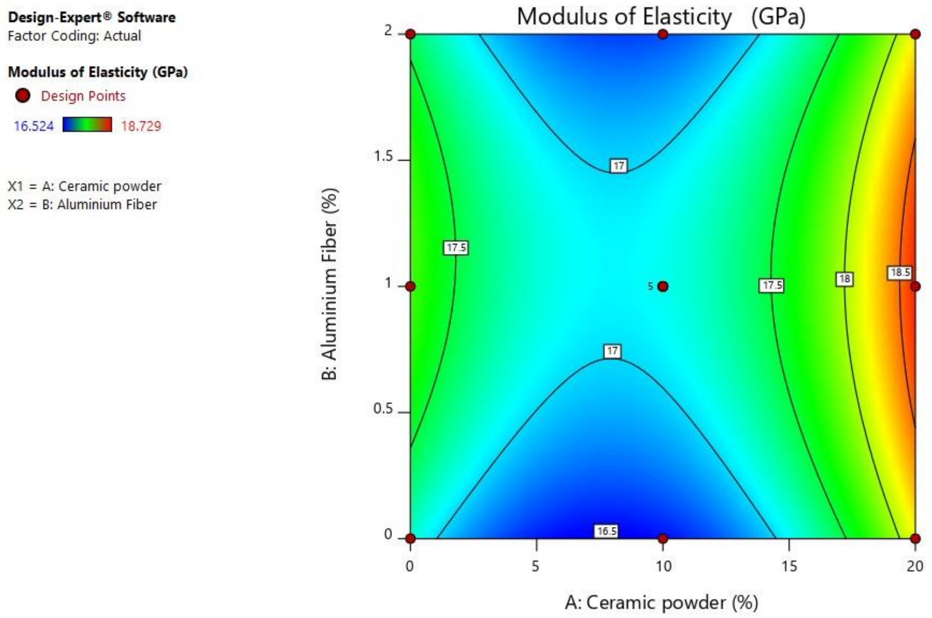
Design-Expert® Software
Factor Coding: Actual
Modulus of Elasticity (GPa)
Design Points
16.524
18.729
X1 = A: Ceramic powder
X2 = B: Aluminium Fiber
Modulus of Elasticity (GPa)
B: Aluminium Fiber (%)
A: Ceramic powder (%)
16.5
17
17.5
18
18.5

(e)

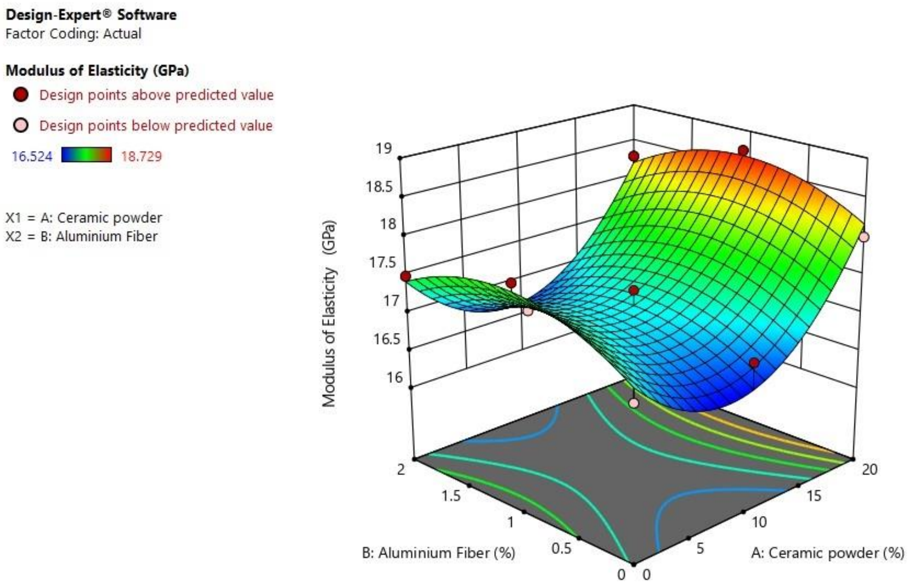
Design-Expert® Software
Factor Coding: Actual
Modulus of Elasticity (GPa)
Design points above predicted value
Design points below predicted value
16.524
18.729
X1 = A: Ceramic powder
X2 = B: Aluminium Fiber
Modulus of Elasticity (GPa)
B: Aluminium Fiber (%)
A: Ceramic powder (%)

(f)

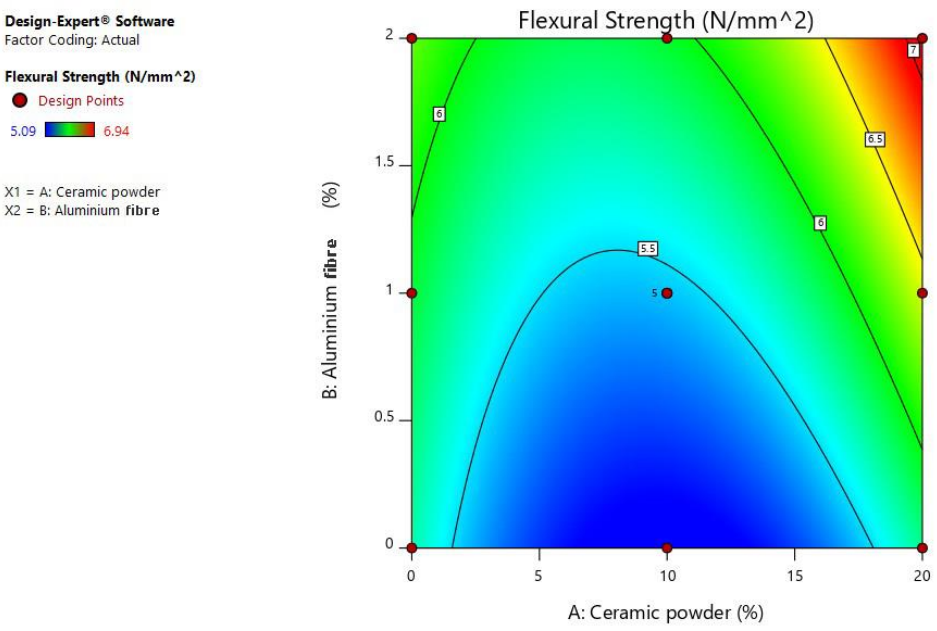
Design-Expert® Software
Factor Coding: Actual
Flexural Strength (N/mm^2)
Design Points
5.09
6.94
X1 = A: Ceramic powder
X2 = B: Aluminium fibre
Flexural Strength (N/mm^2)
B: Aluminium fibre (%)
A: Ceramic powder (%)
5.5
6
6.5
7

(g)

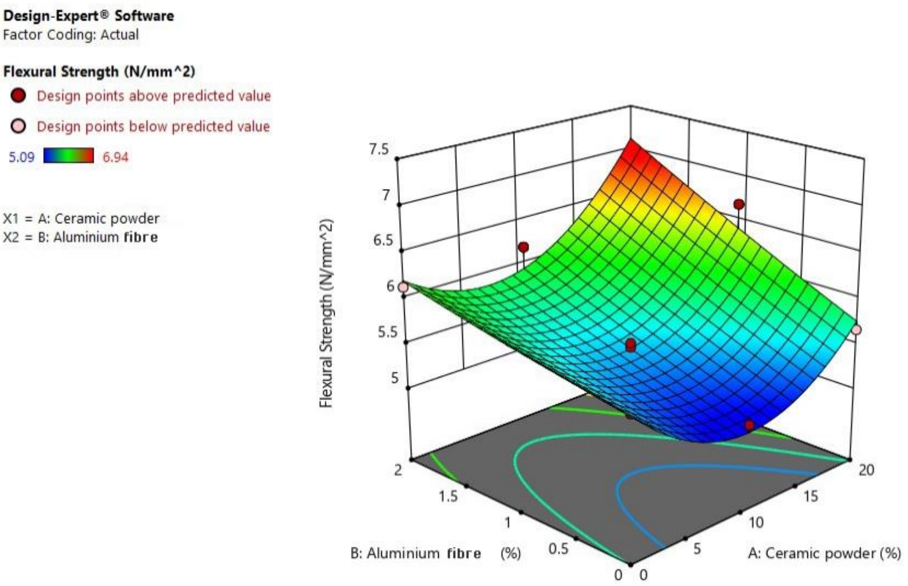

(h)

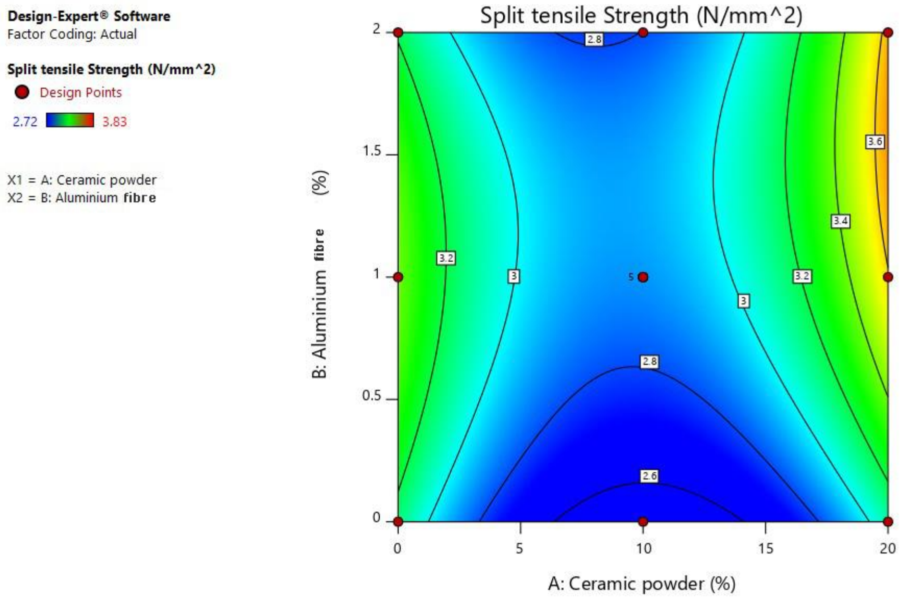

(i)

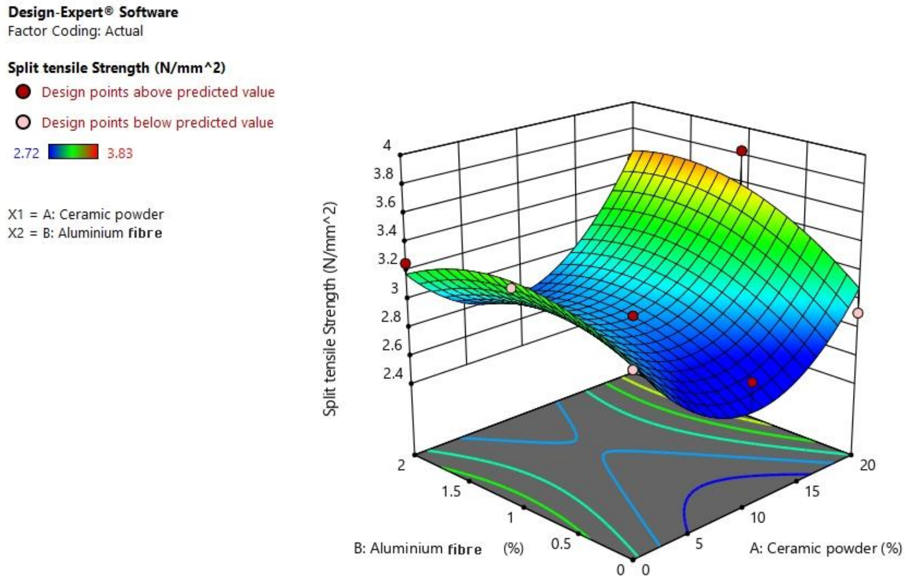

(j)

Figure 7. Contour plot of two variables; aluminum fiber plotted as a function of ceramic Powder

The darker red regions of the contour plot indicate increased strength at different percentage levels, as shown in Figure 7-c. Lighter regions that turn yellow signify intermediary strengths; as the percentage of variables increases in response to either increased or reduced strength, the zones grow darker or lighter. This agrees with Ghayeb et al. [54], who researched predicting the mechanical properties of concrete using intelligent techniques to reduce CO_2 emissions. The RSM model utilising contour plots showed that the red regions of their plot had the maximum increase in strength, and the yellow regions denoted a decrease in strength.

3.3.3. Response Surface Methodology Optimisation

The optimal values for the independent variables (Aluminium fibre and ceramic powder) were determined using the optimisation tool of RSM. The desirable compressive, flexural, and split tensile strengths were defined as being the maximum to attain the highest strength. The desirable slump was defined as being in the range to achieve concrete with good workability. The optimisation yielded many results; however, the results with the highest desirability were taken and presented in Table 11. The process involved interpolating factors within the range considered in the mix design to obtain a response for all properties investigated. A laboratory experiment was conducted using the optimum mix design proportion to validate the model prediction. The results obtained showed that the experimental results were close to those predicted by the models. The absolute relative percent errors (PE) for fibre-reinforced ferroconcrete containing aluminium fibre and ceramic powder were 0.4, 1.2, 1.4, 1.7, and 0.9 for the slump, compressive strength, split tensile strength, flexural strength, and modulus of elasticity, respectively. From the relatively low values obtained for percentage error, it could be deduced that the model forecasted the anticipated responses with good accuracy.

Table 11. Model prediction and validation

	Parameters	Unit	Goal	Model prediction	Laboratory experiment	Percentage Error
Input Parameters	A: Ceramic Powder	%	Maximum	20	20	-
	B: Aluminium Fibre	%	Maximum	1.492	1.492	-
Output Parameters	Slump	mm	In Range	22.032	21.184	0.4
	Compressive Strength	N/mm^2	Maximum	15.581	15.395	1.2
	Modulus of Elasticity	GPa	Maximum	18.548	18.382	0.9
	Flexural Strength	N/mm^2	Maximum	6.750	6.631	1.7
	Split Tensile Strength	N/mm^2	Maximum	3.669	3.618	1.4

Absolute relative per cent error $(\boldsymbol{PE}) = \mathbf{1} - (\frac{ValuePredicted}{ValueExperiment}) \times \mathbf{100}$

3.3.4. Microstructures

Scanning Electron Microscopy (SEM) was used for microstructural analysis. Samples with optimal ceramic powder (20%) and Aluminium fibre (1%), samples with ceramic powder only, and non-fibrous normal concrete were observed under a Variable-Pressure Scanning Electron Microscopy (SEM), JEOL JSM-IT300LV with a working voltage of 20kV. The micrographs indicate the effect of Aluminium Fiber (AF) ceramic powder on the ferroconcrete matrix. The micrograph of mix CP0+ AF0 shown in Figure 8-a reveals some voids on the matrix, though there were CSH formations but not as much as in Figure 8-b. 20% of CP made the microstructure denser due to the filler action of CP and the existence of crystalised C-S-H compared to conventional concrete in Figure 9-a. It could be linked to the enhancement of hydration due to the pozzolanic effect of CP. According to the report by Chindaprasirt & Rukzon [55], additional cementitious materials in concrete composites enhance concrete through a 'filling mechanism'. Figures 9-a and 9-b are micrographs of a mix with CP20+AF1. The microstructure is filled with C-S-H crystal structures and Calcium Sulphate, which likely caused the improved strength of that mixture [56]. However, some cracks were observed on the microstructure due to fibre pull-out.

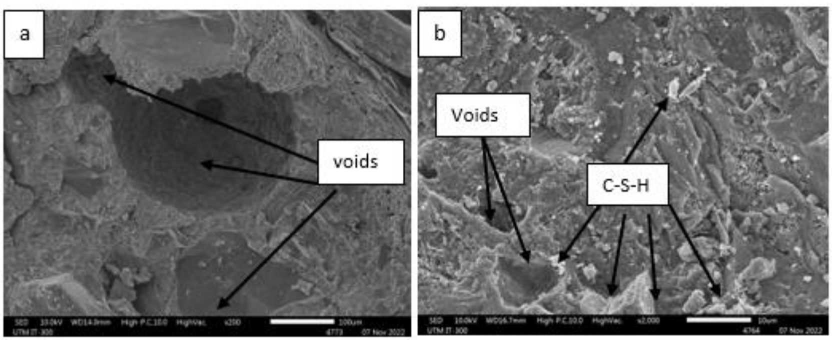

Figure 8. a) Micrograph with CP0 and AF0, b) Micrograph with CP20 and AF0

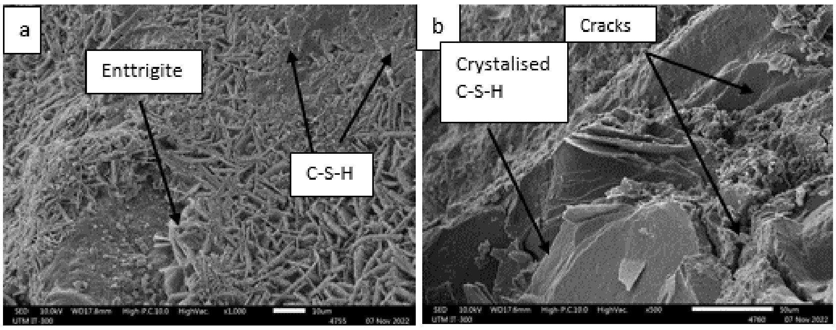

Figure 9. a) Micrograph with CP20 and AF1, b) Micrograph with CP20 and AF1(×2000)

4. Conclusions and Recommendations

Fibre-reinforced ferroconcrete is a new type of lightweight concrete investigated in this research study for improved performance in sustainable construction. The study attempts to evaluate the effect of combining ceramic powder and aluminium fibres in percentages to ascertain if it influences a change in the fresh and mechanical properties of the ferroconcrete. The ceramic powder was used as a partial replacement for cement to reduce demand for cement and decrease the emissions of CO_2 as a result of cement production; aluminium fibres acted as lightweight, eco-friendly reinforcement and possessed an overall average tensile strength. RSM models were produced to reduce time and cost and accurately predict ferroconcrete properties without going through the rigours of laboratory experiments. The predicted data of the RSM show good agreement with the actual results. The outcome of the fibre-reinforced ferroconcrete is concluded as follows:

- The study shows that the combination of aluminium fibre and ceramic powder impedes the fresh properties of the ferroconcrete. Control concrete recorded a slump value of 40mm. With the addition of ceramic powder and aluminium fibre at 10% and 1%, respectively, the slump was reduced to 28mm. Slump values of 35mm and 30 mm were recorded with 10% and 20% replacement of ceramic powder and no fibres, but the lowest slump (18mm) was achieved at 2% addition of aluminium fibres and 20% replacement of ceramic powder. This proves that both aluminium fibre and ceramic powder will produce fibre-reinforced ferroconcrete with low workability. Slump flow can be improved mainly by adding a higher amount of superplasticiser.
- The maximum compressive strength was observed at 20% ceramic powder and 1% aluminium fibre. This showed an increased strength gain of up to 21.59% against control concrete, where ferroconcrete had 15.88 N/mm^2 and control had 13.06 N/mm^2.The grade of concrete is M15, which conforms to the highest compressive strength value.
- The maximum split tensile strength was observed at 20% ceramic powder and 1% aluminium fibre; an increased strength gain of up to 23.15% was recorded where ferroconcrete had a strength of 3.83 N/mm^2 and control had 3.11 N/mm^2. Adding ceramic powder and aluminium fibre provided more toughness to the ferroconcrete.
- The maximum flexural strength was achieved with 20% ceramic powder and 2% aluminium fibre. At 0% ceramic powder and 2% aluminium fibre, the flexural strength gains against control concrete were 7.16%, and at 20% ceramic powder and 2% fibre, the strength further improved to a gain of 21.32%. This confirms that adding aluminium fibres shows improved ductility in the ferroconcrete compared to conventional concrete.
- The effects of the layers of wire mesh on the fibre-reinforced ferroconcrete prove that the ferroconcrete will not entirely rupture on failure. The wire mesh provided more toughness to the ferroconcrete as it seemingly did not break into halves on the impact of maximum loading.
- The Optimised mix design necessary to obtain the best fresh and mechanical properties was deduced to be a 20% proportion of ceramic powder and a 1.68% proportion of aluminium fibres. These combinations produced a slump value of 20.902 mm, compressive strength of 15.376 N/mm^2, flexural strength of 6.886 N/mm^2, and split tensile strength of 3.670 N/mm^2 using the RSM-centered model. This RSM-optimised model showed good accuracy, as the percentage error of the experimental data and predicted data for all experiments did not exceed 1.7%. Therefore, using this model is recommended for engineering applications.
- The RSM model results show that the coefficient of determination (R^2) tends to be 1, with values of 0.9518, 0.9172, 0.9328, and 0.8843 for the slump, compressive strength, flexural strength, and split tensile strength, respectively. Aside from split tensile strength, which shows an 88% accuracy ratio, the R^2 values for other experiments showed an accuracy of more than 90%, which affirms that the model is adequate for the perfect imitation of the investigated characteristics of fibre-reinforced ferroconcrete.

Fibre-reinforced ferroconcrete has been proven to have improved performance through various mechanical tests. However, it faces limitations such as very low workability, which makes it unsuitable for beam and column structural work. However, it possesses good flexural strength, which can find applications in slab work, concrete walls, and pavements. For further studies, these can present new knowledge:

- Aluminium fibres of greater tensile strength can be considered for use.
- Aluminium fibres were obtained from external layers of armoured cables that find use in electrical applications; other sources of aluminium fibres can be investigated.
- Similarly, linking chains of fibres rather than randomly dispersing them could also prove effective.
- A comparison between models like the artificial neural network and response surface methodology can be utilised to check each model's degree of efficiency and determine which model has better simulation and optimisation properties.

5. Declarations

5.1. Author Contributions

Conceptualization, T.F.A., A.I.E., O.O.A., A.M., and A.F.D.; methodology, T.F.A., A.I.E., O.O.A., A.M., and A.F.D.; formal analysis, T.F.A., A.I.E., O.O.A., A.M., and A.F.D.; data curation, T.F.A., A.I.E., O.O.A., A.M., and A.F.D.; writing—original draft preparation, O.G.A.; writing—review and editing, T.F.A., A.I.E., O.O.A., A.M., A.F.D., and O.G.A. All authors have read and agreed to the published version of the manuscript.

5.2. Data Availability Statement

The data presented in this study are available in the article.

5.3. Funding

The authors received no financial support for the research, authorship, and/or publication of this article.

5.4. Acknowledgements

The authors would like to acknowledge all the staff at the Civil Engineering Laboratory of Afe Babalola University, Ado Ekiti, Nigeria, for their immense support during the laboratory work. The management of Afe Babalola University is also appreciated for its financial contribution to ensuring the accessibility of this research output.

5.5. Conflicts of Interest

The authors declare no conflict of interest.

6. References

[1] Fahmy, E. H., Shaheen, Y. B. I., Abdelnaby, A. M., & Abou Zeid, M. N. (2014). Applying the Ferrocement Concept in Construction of Concrete Beams Incorporating Reinforced Mortar Permanent Forms. International Journal of Concrete Structures and Materials, 8(1), 83–97. doi:10.1007/s40069-013-0062-z.

[2] Karthik, M. P., & Maruthachalam, D. (2015). Experimental study on shear behaviour of hybrid Fibre Reinforced Concrete beams. KSCE Journal of Civil Engineering, 19(1), 259–264. doi:10.1007/s12205-013-2350-1.

[3] Dhilip Kumar, R. G., Sukumar, B., Hemamathi, A., Ram Shankar, P., & Balki, S. (2021). Experimental investigation on Ferrocement slab using partial replacement of cement by ceramic powder. Journal of Physics: Conference Series, 2070(1), 012195. doi:10.1088/1742-6596/2070/1/012195.

[4] Kannan, D. M., Aboubakr, S. H., EL-Dieb, A. S., & Reda Taha, M. M. (2017). High performance concrete incorporating ceramic waste powder as large partial replacement of Portland cement. Construction and Building Materials, 144, 35–41. doi:10.1016/j.conbuildmat.2017.03.115.

[5] Subaşı, S., Öztürk, H., & Emiroğlu, M. (2017). Utilising of waste ceramic powders as filler material in self-consolidating concrete. Construction and Building Materials, 149, 567–574. doi:10.1016/j.conbuildmat.2017.05.180.

[6] Rawat, R., Singh, A., & Bohra, M. (2019). Investigation of Ceramic Waste as Supplementary Cementitious Material in Concrete. International Journal of Applied Engineering Research, 14(9), 20–25.

[7] Steiner, L. R., Bernardin, A. M., & Pelisser, F. (2015). Effectiveness of ceramic tile polishing residues as supplementary cementitious materials for cement mortars. Sustainable Materials and Technologies, 4, 30–35. doi:10.1016/j.susmat.2015.05.001.

[8] Jackiewicz-Rek, W., Załęgowski, K., Garbacz, A., & Bissonnette, B. (2015). Properties of cement mortars modified with ceramic waste fillers. Procedia Engineering, 108, 681–687. doi:10.1016/j.proeng.2015.06.199.

[9] Awoyera, P. O., Dawson, A. R., Thom, N. H., & Akinmusuru, J. O. (2017). Suitability of mortars produced using laterite and ceramic wastes: Mechanical and microscale analysis. Construction and Building Materials, 148, 195–203. doi:10.1016/j.conbuildmat.2017.05.031.

[10] Rawat, S., & Daverey, A. (2018). Characterisation of household solid waste and current status of municipal waste management in Rishikesh, Uttarakhand. Environmental Engineering Research, 23(3), 323-329. doi:10.4491/eer.2017.175.

[11] El-Gamal, S. M. A., El-Hosiny, F. I., Amin, M. S., & Sayed, D. G. (2017). Ceramic waste as an efficient material for enhancing the fire resistance and mechanical properties of hardened Portland cement pastes. Construction and Building Materials, 154, 1062–1078. doi:10.1016/j.conbuildmat.2017.08.040.

[12] Halicka, A., Ogrodnik, P., & Zegardlo, B. (2013). Using ceramic sanitary ware waste as concrete aggregate. Construction and Building Materials, 48, 295–305. doi:10.1016/j.conbuildmat.2013.06.063.

[13] Chen, X., Zhang, D., Cheng, S., Xu, X., Zhao, C., Wang, X., Wu, Q., & Bai, X. (2022). Sustainable reuse of ceramic waste powder as a supplementary cementitious material in recycled aggregate concrete: Mechanical properties, durability and microstructure assessment. Journal of Building Engineering, 52, 104418. doi:10.1016/j.jobe.2022.104418.

[14] Rajaraman, J. (2017). Study on structural behavior of aluminium fiber in concrete. Journal of Engineering and Applied Sciences, 12(11), 9182-9183. doi:10.36478/jeasci.2017.9182.9183.

[15] Sabapathy, Y. K., Sabarish, S., Nithish, C. N. A., Ramasamy, S. M., & Krishna, G. (2021). Experimental study on strength properties of aluminium fibre reinforced concrete. Journal of King Saud University - Engineering Sciences, 33(1), 23–29. doi:10.1016/j.jksues.2019.12.004.

[16] Muwashee, R. S., Al-Jameel, H. A., & Jabal, Q. A. (2018). Investigating the behavior of concrete and mortar reinforced with aluminum waste strips. International Journal of Engineering and Technology, 7(4), 211–213. doi:10.14419/ijet.v7i4.37.24103.

[17] Rita, B., & Lauren Fraser, R. M. (2018). Exploring the Properties of Fiber Reinforced Concrete. February 2018, 1–48. Available online: http://www.wpi.edu/Academics/Projects (accessed on March 2023).

[18] Pakravan, H. R., Latifi, M., & Jamshidi, M. (2017). Hybrid short fiber reinforcement system in concrete: A review. Construction and Building Materials, 142, 280–294. doi:10.1016/j.conbuildmat.2017.03.059.

[19] Zhang, P., Han, S., Ng, S., & Wang, X.-H. (2018). Fiber-Reinforced Concrete with Application in Civil Engineering. Advances in Civil Engineering, 2018, 1–4. doi:10.1155/2018/1698905.

[20] Channa, I. A., & Saand, A. (2021). Mechanical behavior of concrete reinforced with waste aluminium strips. Civil Engineering Journal (Iran), 7(7), 1169–1182. doi:10.28991/cej-2021-03091718.

[21] Sarabia, L. A., & Ortiz, M. C. (2009). Response Surface Methodology. Comprehensive Chemometrics, 345–390, John Wiley & Sons, Hoboken, United States. doi:10.1016/B978-044452701-1.00083-1.

[22] Upasani, R. S., & Banga, A. K. (2004). Response surface methodology to investigate the iontophoretic delivery of tacrine hydrochloride. Pharmaceutical Research, 21(12), 2293–2299. doi:10.1007/s11095-004-7682-6.

[23] Awolusi, T. F., Oke, L. O., Akinkurolere, O. O., Ubani, D. P., Bamisaye, R. T., & Aluko, O. G. (2021). The Application of Response Surface Methodology in Understanding the Compressive Strength and Water Absorption Capacity of Sandcrete Blocks. Silicon, 13(11), 4123–4132. doi:10.1007/s12633-020-00701-0.

[24] Song, H., Ahmad, A., Ostrowski, K. A., & Dudek, M. (2021). Analysing the compressive strength of ceramic waste-based concrete using experiment and artificial neural network (Ann) approach. Materials, 14(16). doi:10.3390/ma14164518.

[25] Akhtar, J. N., Ahmad, T., Akhtar, M. N., & Abbas, H. (2014). Influence of Fibers and Fly Ash on Mechanical Properties of Concrete. American Journal of Civil Engineering and Architecture, 2(2), 64–69. doi:10.12691/ajcea-2-2-2.

[26] Yu, R., Tang, P., Spiesz, P., & Brouwers, H. J. H. (2014). A study of multiple effects of nano-silica and hybrid fibres on the properties of Ultra-High Performance Fibre Reinforced Concrete (UHPFRC) incorporating waste bottom ash (WBA). Construction and Building Materials, 60, 98–110. doi:10.1016/j.conbuildmat.2014.02.059.

[27] Manasa, B., Sowmyashree, T., & Khedagi, S. B. (2018). Experimental Studies on Behaviour of Ferroconcrete Beams. International Journal of Research in Engineering and Technology, 07(03), 28–33. doi:10.15623/ijret.2018.0703005.

[28] ASTM C150/C150M-22. (2022). Standard Specification for Portland Cement. ASTM International, Pennsylvania, United States. doi:10.1520/C0150_C0150M-22.

[29] BS EN 12620. (2013). Aggregates for concrete. British Standards Institution, London, United Kingdom.

[30] BS EN 206. (2013). Concrete - specification, performance, production and conformity. British Standards Institution, London, United Kingdom.

[31] Wan Hassan, W. N. F., Ismail, M. A., Lee, H.-S., Meddah, M. S., Singh, J. K., Hussin, M. W., & Ismail, M. (2020). Mixture optimisation of high-strength blended concrete using central composite design. Construction and Building Materials, 243, 118251. doi:10.1016/j.conbuildmat.2020.118251.

[32] BS EN 12350-2. (2009). Testing fresh concrete. Slump-test. British Standards Institution, London, United Kingdom.

[33] ASTM C349-18. (2018). Standard Test Method for Compressive Strength of Hydraulic Cement Mortars (Using Portions of Prisms broken in Flexure). ASTM International, Pennsylvania, United States. doi:10.1520/C0349-18.

[34] BS EN 12390-6. (2009). Testing hardened concrete. Tensile splitting strength of test specimens. British Standards Institution, London, United Kingdom.

[35] ASTM C348-21. (2021). Standard Test Method for Flexural Strength of Hydraulic Cement. ASTM International, Pennsylvania, United States. doi:10.1520/C0348-21.

[36] ACI-318-14. (2014). Building Code Requirement for Structural Concrete. American Concrete Institute (ACI), Michigan, United States.

[37] BS EN 12350-2. (2009). Testing fresh concrete. Slump-test. British Standards Institution, London, United Kingdom.

[38] Cheng, Y., Huang, F., Liu, R., Hou, J., & Li, G. (2015). Test research on effects of waste ceramic polishing powder on the permeability resistance of concrete. Materials and Structures, 49(3), 729–738. doi:10.1617/s11527-015-0533-6.

[39] Zeyad, A. M. (2020). Effect of fibers types on fresh properties and flexural toughness of self-compacting concrete. Journal of Materials Research and Technology, 9(3), 4147–4158. doi:10.1016/j.jmrt.2020.02.042.

[40] Kanag, S. Y., Anandan, Y. K., Vaidyanath, P., & Baskar, P. (2016). Strength properties of coated E-glass fibres in concrete. Gradjevinar, 68(9), 697–703. doi:10.14256/JCE.1335.2015.

[41] Kiran, T. S., & Rao, K. S. (2016). Mechanical Properties of Glass Fiber Reinforced Concrete. International Journal of Civil and Structural Engineering Research, 3(2), 164–173.

[42] Datye, P. P., & Pawar, S.S. (2015). Experimental Approach to assess the viability of Aluminium Matrix Composites in Concrete. International Journal of Innovative Research in Science, Engineering and Technology, 4(9), 9035-9038. doi:10.15680/IJIRSET.2015.0409104.

[43] Shao, R., Wu, C., Li, J., & Liu, Z. (2022). Development of sustainable steel fibre-reinforced dry ultra-high performance concrete (DUHPC). Journal of Cleaner Production, 337, 130507. doi:10.1016/j.jclepro.2022.130507.

[44] Liu, Z., Worley II, R., Du, F., Giles, C. D., Dewoolkar, M., Huston, D., & Tan, T. (2021). A study on avalanches of early age basalt fiber reinforced concrete beams during flexure. Journal of Cleaner Production, 279, 123695. doi:10.1016/j.jclepro.2020.123695.

[45] Lazorenko, G., Kasprzhitskii, A., & Fini, E. H. (2022). Polyethylene terephthalate (PET) waste plastic as natural aggregate replacement in geopolymer mortar production. Journal of Cleaner Production, 375, 134083. doi:10.1016/j.jclepro.2022.134083.

[46] Ravinder, K. (2016). Strength Characteristics of Coca-Cola Tin Waste As Fibres in Concrete. International Journal of Advanced Research Foundation, 3(2), 9–12.

[47] Ilya, J., & Cheow Chea, C. (2017). Mechanical behaviour of fibre reinforced concrete using soft – drink can. IOP Conference Series: Materials Science and Engineering, 271, 012079. doi:10.1088/1757-899x/271/1/012079.

[48] Parida, A., Sarangi, S., & Jayashree, B. (2017). Study the modulus elasticity of HFRC. Journal of Industrial Pollution Control, 33(1), 1209–1213.

[49] Sagar, B., & Sivakumar, M. V. N. (2021). Performance evaluation of basalt fibre-reinforced polymer rebars in structural concrete members–a review. Innovative Infrastructure Solutions, 6, 1-18. doi:10.1007/s41062-020-00452-2.

[50] Talib, N. A. A., Salam, F., Yusof, N. A., Alang Ahmad, S. A., & Sulaiman, Y. (2017). Optimisation of peak current of poly(3,4-ethylenedioxythiophene)/multi-walled carbon nanotube using response surface methodology/central composite design. RSC Advances, 7(18), 11101–11110. doi:10.1039/c6ra26135c.

[51] Awolusi, T. F., Oke, O. L., Akinkurolere, O. O., Sojobi, A. O., & Aluko, O. G. (2019). Performance comparison of neural network training algorithms in the modeling properties of steel fiber reinforced concrete. Heliyon, 5(1). doi:10.1016/j.heliyon.2018.e01115.

[52] Schober, P., & Schwarte, L. A. (2018). Correlation coefficients: Appropriate use and interpretation. Anesthesia and Analgesia, 126(5), 1763–1768. doi:10.1213/ANE.0000000000002864.

[53] Pomerantsev, A. L., & Rodionova, O. Y. (2010). Chemometric view on "comprehensive chemometrics". Chemometrics and Intelligent Laboratory Systems, 103(1), 19-24. doi:10.1016/j.chemolab.2010.05.001.

[54] Ghayeb, H. H., Razak, H. A., Sulong, N. H. R., Hanoon, A. N., Abutaha, F., Ibrahim, H. A., Gordan, M., & Alnahhal, M. F. (2019). Predicting the mechanical properties of concrete using intelligent techniques to reduce CO_2 emissions. Materiales de Construccion, 69(334), 0465–2746. doi:10.3989/mc.2019.07018.

[55] Chindaprasirt, P., & Rukzon, S. (2015). Strength and chloride resistance of the blended Portland cement mortar containing rice husk ash and ground river sand. Materials and Structures/Materiaux et Constructions, 48(11), 3771–3777. doi:10.1617/s11527-014-0438-9.

[56] Lasseuguette, E., Burns, S., Simmons, D., Francis, E., Chai, H. K., Koutsos, V., & Huang, Y. (2019). Chemical, microstructural and mechanical properties of ceramic waste blended cementitious systems. Journal of Cleaner Production, 211, 1228–1238. doi:10.1016/j.jclepro.2018.11.240.